Nuclear Engineering and Design 239 (2009) 728–734

Contents lists available at ScienceDirect

Nuclear Engineering and Design

journal homepage: www.elsevier.com/locate/nucengdes

Modeling liquid–gas iodine mass transfer under evaporative conditions during severe accidents

L.E. Herranz [a,*], J. Fontanet [a], L. Cantrel [b]

[a] Unit of Nuclear Safety Research, CIEMAT, Avda. Complutense 22, 28040 Madrid, Spain
[b] Institut de Radioprotection et de Surete Nucléaire, Direction de la Prévention des Accidents Majeurs, SEMIC, LETR, Cadarache, Bat 702, F-13115 Saint Paul lez Durance, France

ARTICLE INFO

Article history:
Received 4 June 2008
Received in revised form 14 January 2009
Accepted 18 January 2009

ABSTRACT

During postulated severe accidents transfer of volatile iodine dissolved in containment water sumps to atmosphere can be fostered under pool evaporative conditions. Scarcity of representative data has resulted in semi-empirical models that relies on fitting parameters and still need of further validation. This paper presents a mechanistic model based on: the two-film model, the heat-mass transfer analogy and the surface renewal theory. Comparison to data from the SISYPHE program, performed at the French "Institut de Radioprotection et de Sûreté Nucléaire", has resulted in an accurate response, the error band being 9–25% for the aqueous steady state concentration. Likewise, the model performance has been compared to the model implemented in the ASTEC code. In addition to yield similar results, some advantages have been highlighted: the mechanistic nature, the estimates conservatism, and the thorough documentation of model grounds and assumptions.

1. Introduction

Water phase changes play a key role in the evolution of postulated severe accidents within nuclear power plant containments. Pressure evolution is conditioned to a large extent by water steaming (either from the primary circuit or from liquid ponds set up in containment) and steam condensation. Given its nature as a passive safety mechanism, steam condensation onto in-containment surfaces in the presence of non-condensable gases has been profusely investigated within the nuclear safety community and thorough reviews may be found in literature (Green and Almenas, 1996; de la Rosa et al., 2008). Nonetheless, steaming from liquid pools can also play a major role in severe accident scenarios as a driving mechanism for some volatile species transfer between sump and atmosphere.

Many postulated severe accidents develop in such a way that a large aqueous sump builds up at the bottom of containment due to the water input from the reactor coolant system and/or from water-injecting safety systems. As most of fission products, except for noble gases and a certain fraction of iodine, enter containment in particulate form, they are eventually dragged into the sump, either directly by gravity or indirectly from surface draining effect (Herranz et al., 2007). The fission products decay would deliver their residual heat to the water and it could drive the containment sump to an evaporative thermal state, making a fraction of the inventory turn into steam and get transported to the atmosphere. Thus, an evaporative sump would yield a higher steam fraction in the containment atmosphere and, no less important, it would also enhance transfer of volatile fission products from sump to atmosphere. This latter effect would enlarge source term in case of loosing containment leak-tightness. The radiological implications of isotope 131 of iodine and the volatility of some of its chemical species, make iodine mass transfer enhancement a potentially important safety issue.

Existing data base on in-containment sump-to-atmosphere iodine mass transfer under evaporative conditions is scarce and less representative than what would be desirable. SISYPHE (Verloo et al., 1998), EPICUR (IRSN et al., 2004) and PHEBUS-FP (Schwarz and Zeyen, 2003) projects (conducted by IRSN under international frameworks) have intended to fix this situation. Such lack of data results in models susceptible to be improved and fully validated. Most of existing models in codes are based on the two-film theory (Perry and Green, 1997), which does not consider any phase change at the gas–liquid interface assuming that volatile species reach equilibrium at the interface. As a consequence, their predictions accuracy is not satisfactory under conditions other than purely convective ones. An extension of the two-film model has been successfully developed and compared to available data (Cantrel and March, 2006); however, the parametric approach of this adaptation leaves room for developing a more mechanistically based model.

This paper shows the potential impact of evaporation on in-containment source term and presents a two-film based model

* Corresponding author. Tel.: +34 913466219; fax: +34 913466233.
E-mail addresses: luisen.herranz@ciemat.es (L.E. Herranz), joan.fontanet@ciemat.es (J. Fontanet), laurent.cantrel@irsn.fr (L. Cantrel).

0029-5493/$ – see front matter © 2009 Elsevier B.V. All rights reserved.
doi:10.1016/j.nucengdes.2009.01.006

Nomenclature

a	scaling constant
A	surface area
C	concentration of species
D	diffusion coefficient
g	gravity constant
Gr	Grashof number
H	partition coefficient
k	individual mass transfer coefficient
L	characteristic length
$\dot{m}_{ev}$	evaporation rate
M	molar weight
P	pressure
R	ideal gases constant
Sc	Schmidt number
Sh	Sherwood number
T	temperature
U	wind velocity near the water surface
U^*	friction velocity

Greek symbols

δ	boundary layer thickness
ε	rate of turbulent energy dissipation
μ	dynamic viscosity
ν	kinematic viscosity
ρ	density
σ	characteristic length parameter
φ	mass flow rate
Ω_D	collision integral for diffusion

Subscripts and superscripts

bulk	gas bulk
cond	condensers
d	drift component of the energy dissipation
g	gas phase
i	volatile species
I2	iodine
int	interface
ℓ	liquid phase
s	mechanical mixing component of the energy dissipation
sat	steam at saturation condition
H2Ov	steam
nc	non-condensable gases
w	wave component of the energy dissipation

extended to phase change conditions on the heat-mass transfer analogy at the gas phase and on a correlation based on the surface renewal theory at the liquid side. Its predictions are compared to the experimental data available from the SISYPHE project and to estimates from the parametric model mentioned above, which was implemented in the IODE module of the ASTEC code. This work has been carried out under the frame of the SARNET project of the 6th Framework Programme of EURATOM (Haste et al., 2006).

2. Assessment of evaporation impact

In order to assess the potential effect of evaporation on the in-containment source term two theoretical studies have been carried out. The former investigates the change of the liquid-to-gas concentration ratio of iodine at steady state with respect to non-evaporative scenarios. The latter proposes a simplified evaporative in-containment scenario and explores how differently gaseous iodine would evolve as evaporation is accounted for in the modeling.

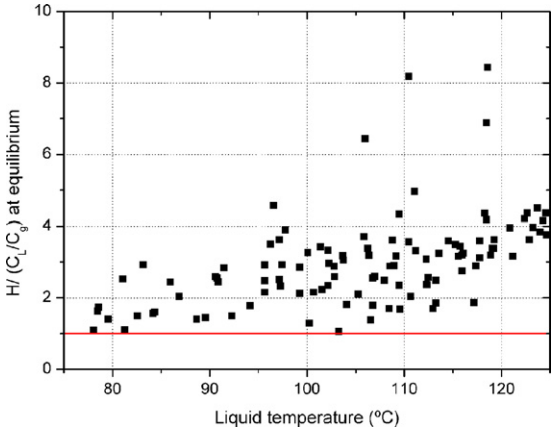

Fig. 1. Effect of evaporation on the equilibrium partition of iodine.

The primary variables influencing evaporation can be reduced to a small group of magnitudes: liquid and gas temperatures, pressure and relative humidity. By randomly choosing specific values within the ranges of interest (T_ℓ, 75–125 °C; T_g, 75–125 °C; P, 1.0–5.0 bar; RH, 25–100%), more than 100 thermal scenarios have been defined. As will be shown in next sections, the ratio between the iodine partition coefficient (H) and the actual liquid-to-gas concentration ratio can be calculated as:

$$\frac{H}{C_\ell/C_g} = 1 + \frac{\dot{m}_{ev}}{A_{int}\ \rho_{sat}(T_\ell)k_g} \quad (1)$$

The results obtained are shown in Fig. 1. A few cases show that under evaporative conditions the concentration ratio between liquid and gas might even reach values around 8 times lower than what would be predicted under non-evaporative conditions. Anyway, most of the scenarios calculated show C_ℓ/C_g values between 2 and 4 times smaller than under pure convective conditions. In other words, evaporation would generally result in a concentration steady state characterized by a gaseous iodine concentration over twice the one resulting under non-evaporative conditions.

By using the ASTEC code (Van Dorsseleare and Schwinges, 2005) a postulated containment scenario has been simulated. The thermal and chemical conditions (Table 1), even though within the range anticipated in case of a severe accident, have been chosen to maximize the effect of evaporation. The resulting evaporation flux is around 8×10^{-3} kg m^{-2} s^{-1} and the pH is low enough to let molecular iodine (I_2) to be formed from the initial I^- solution (10^{-5} M) by radiolysis. In order not to include chemical processes highly uncertain at present (i.e., organic chemistry, gaseous oxidation of iodine,

Table 1
Postulated conditions for a containment severe accident scenario.

Variable	Value
Geometry	
Containment volume	50,000 m^3
Sump volume	2,100 m^3
TH condition	
Sump temperature	~122 °C
Initial wall temperature	50 °C
Gas temperature	~87 °C
Total pressure	2.3 bar
Steam pressure	0.62 bar
Chemical conditions	
pH	5
Dose rate	2.5 Gy/s
Initial I^- concentration	10^{-5} kmol/m^3

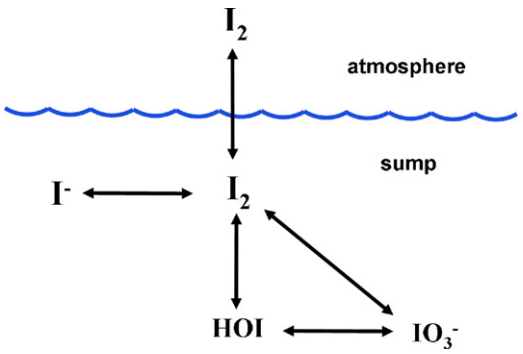

Fig. 2. Iodine chemistry model to assess evaporation.

adsorption/desorption processes, etc.), a simplified inorganic scenario has been assumed as the one governing iodine chemistry and liquid–gas exchange (Fig. 2).

As may be observed in Fig. 3, iodine gas concentration increases to a substantial higher level under evaporative conditions (around a factor of 8) and, in addition, the steady state is reached at far longer times than under convection due to a higher gaseous iodine concentration.

In short, the above studies have shown the potential for evaporation to enhance mass transfer of iodine from an aqueous sump to the gas phase over it. The change is quantitatively significant, so that inclusion of an evaporative mass transport model is worthwhile.

3. Model description

3.1. Fundamentals

Under evaporative conditions, the volatile iodine within the aqueous solution will be transferred to the atmosphere by two mechanisms:

- Diffusion (i.e., transport due to iodine concentration gradients).
- Dragging by the steam flow from the liquid–gas interface (i.e., proportional to evaporation rate).

By adopting the double boundary layer approach of the two-film theory (Fig. 4), the gaseous and liquid mass flow rates may be written as:

$$\varphi_g = -A_{int} k_g (C_g - C_g^{int}) + \frac{\dot{m}_{ev}}{\rho_{sat}(T_\ell)} C_g^{int} \quad (2)$$

$$\varphi_\ell = -A_{int} k_\ell (C_\ell^{int} - C_\ell) \quad (3)$$

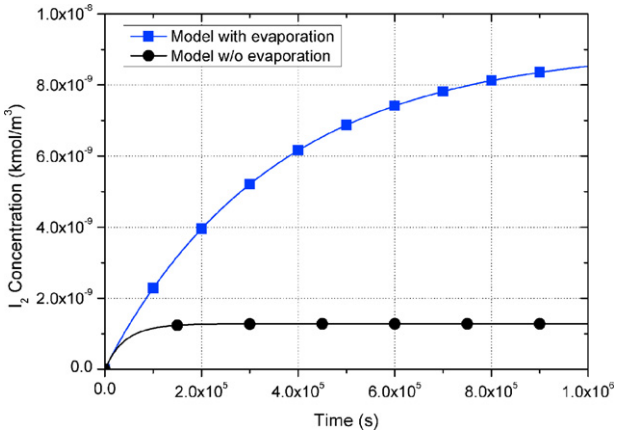

Fig. 3. Gaseous I_2 concentration in a postulated accident scenario.

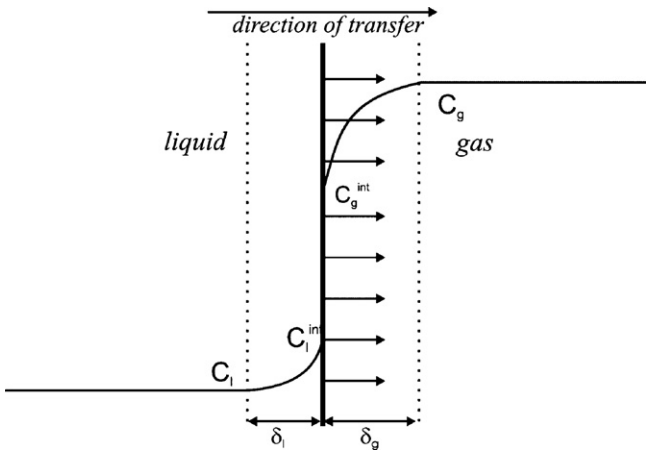

Fig. 4. Sketch of the two-film model.

These equations implicitly assume that the shrinkage of the liquid side boundary layer due to evaporation has a negligible effect on the whole iodine mass transport. In other words, the main influence of evaporation is driven by sweeping iodine at the gas side of the boundary layer into the gas bulk.

As the interfacial concentrations relate each other through the equilibrium partition coefficient (H):

$$H = \frac{C_\ell^{int}}{C_g^{int}} \quad (4)$$

the balance between gas and liquid mass flow rates at the interface ($\varphi_g = \varphi_\ell$) allows deriving an expression for the iodine gas concentration:

$$C_g^{int} = \frac{k_g C_g + k_\ell C_\ell}{H k_\ell + k_g + (\dot{m}_{ev}/(A_{int}\rho_{sat}(T_\ell)))} \quad (5)$$

that, once included in Eq. (2), yields the following expression for the iodine mass flow rate:

$$\varphi = A_{int}\left(\frac{k_g k_\ell}{k_g + H k_\ell + (\dot{m}_{ev}/(A_{int}\rho_{sat}(T_\ell)))}\right) \times \left(H C_g - \left(1 + \frac{\dot{m}_{ev}}{A_{int}\rho_{sat}(T_\ell) k_g}\right)\cdot C_\ell\right) \quad (6)$$

Then, the iodine concentrations ratio defining the equilibrium condition ($\varphi = 0$) would be:

$$\frac{C_\ell}{C_g} = \frac{H}{1 + (\dot{m}_{ev}/(A_{int}\rho_{sat}(T_\ell) k_g))} \quad (7)$$

This equation shows the consistency of the model since in the absence of evaporation, equilibrium is characterized by the iodine partition coefficient, whereas under evaporation conditions the liquid-to-gas equilibrium concentration ratio decreases. Note that Eq. (1) is just a rearrangement of Eq. (7).

3.2. Mass transfer coefficients

As shown in Eqs. (6) and (7), gas and liquid mass transfer coefficients (i.e., k_g and k_ℓ) are key variables to assess iodine flow rate.

The gas mass transfer coefficient:

$$k_{g,I2} = \frac{D_{g,I2}}{\delta_{g,I2}} \quad (8)$$

can be calculated by an approximate estimate of the iodine boundary layer thickness ($\delta_{g,I2}$). Under anticipated natural convection conditions, the Rayleigh dimensionless number ($Ra = Gr \times Pr$) is

higher than 10^7, so that one may write (Incropera and Dewitt, 2002):

$$\delta_{g,I2} \cong \delta_{g,H2Ov}\left(\frac{Sc_{g,I2}}{Sc_{g,H2Ov}}\right)^{-1/3} = \delta_{g,H2Ov}\left(\frac{D_{g,I2}}{D_{g,H2Ov}}\right)^{1/3} \quad (9)$$

If the steam boundary layer thickness is written in terms of the Sherwood dimensionless number (Sh) and the resulting expression substituted in Eq. (8), it yields:

$$k_{g,I2} = (D_{g,I2}^2 D_{g,H2Ov})^{1/3}\frac{Sh_{H2Ov}}{L} \quad (10)$$

By assuming that heat and mass transfer analogy may be applied, the Sh number may be estimated as (natural convection):

$$Sh_{H2Ov} = 0.15(Gr\,Sc_g)^{1/3}_{H2Ov} \quad (11)$$

Hence, the resulting expression for $k_{g,I2}$ is:

$$k_{g,I2} = \frac{0.15}{L}(D_{g,I2}^2 D_{g,H2Ov})^{1/3}(Gr\,Sc_g)^{1/3}_{H2Ov} \quad (12)$$

By substituting the Grashof ($Gr = |gL^3\rho_{g,bulk}((\rho_{g,int} - \rho_{g,bulk})/\mu_g^2)|$) and Schmidt ($Sc_g = \mu_g/(\rho_g D_g)$) definitions into Eq. (12), one obtains a quite simple equation where $k_{g,I2}$ is observed to depend on the iodine diffusivity in the gas phase and on the steam density difference between the interface and the gas bulk:

$$k_{g,I2} = 0.15 D_{g,I2}^{2/3}\left(\frac{g\,\Delta\rho}{\mu}\right)^{1/3}_{H2Ov} \quad (13)$$

The iodine gas diffusivity in Eq. (13) is estimated by (Reid et al., 1988):

$$D_{g,i} = 8.4\times10^{-24}\times\frac{T_g^{3/2}}{P_g M_{i-g}^{1/2}\sigma_{i-g}^2\Omega_D} \quad (14)$$

Experimental data needed for the collision integral, Ω_D, and the characteristic length (σ) are reported in (Reid et al., 1988).

Concerning k_ℓ, the surface renewal theory suggests that the gas–liquid friction at the interface may contribute significantly to the mass transfer enhancement (Cohen et al., 1978; Emerson, 1975; Kanwisher, 1963). Cohen (1983) derived a correlation of k_ℓ as a function of the water Schmidt number and the individual contributions to the total rate of energy dissipation near the surface:

$$k_{\ell,I2} = a\ Sc_{\ell,I2}^{1/2}[\nu(\varepsilon_d + \varepsilon_w + \varepsilon_s)]^{1/4} \quad (15)$$

As ε_d and ε_w depend on the friction velocity (U^*), and this in turn can be estimated as a function of the gas velocity over the water surface ($U^* = 34.3\,U$) (Wu, 1980), an easier-to-use correlation was proposed:

$$k_{\ell,I2} = Sc_{\ell,I2}^{-1/2}\cdot\left[1.48\times10^{-4} + 4.8\times10^{-4}\left(\frac{U}{0.029}\right)^{1.015}\right] \quad (16)$$

Eq. (16) assumes that the liquid phase is well mixed. Nonetheless, it would be still valid for no well-mixed water bodies if the first term in the squared brackets (1.48×10^{-4}) is substituted for 2.9×10^{-5}. This correlation was validated against experimental data covering a wide range of fluids.

4. Model validation

Even though several recent projects in the arena of severe accident have dealt with mass transfer – i.e., SISYPHE (Verloo et al., 1998), EPICUR (IRSN et al., 2004) and PHEBUS-FP (Schwarz and Zeyen, 2003) – SISYPHE is the only one which specifically investigates the matter. Their results (Cantrel and March, 2006) have been made available through the EU SARNET project and they have been the subject addressed by the so-called mass transfer interpretation circle (MAT). This paper, particularly the next sections, summarizes to a good extent the major achievements accomplished under such a framework.

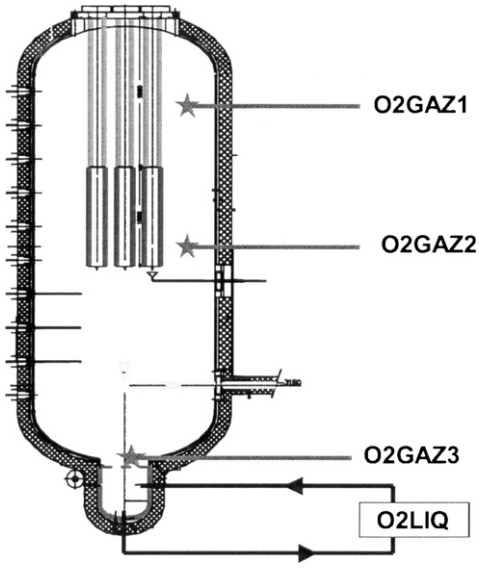

Fig. 5. SISYPHE facility and main instrumentation (Cantrel, 2005a).

4.1. Experimental data

The SISYPHE facility resembles the well-know PHEBUS-FP containment vessel (Shepherd et al., 1995). It consists of a 10 m^3 stainless steel vessel containing three cylindrical condensing surfaces kept at temperatures under saturation. The vessel walls are neutralized (i.e., heated-up above saturation temperature) to avoid on-walls condensation. This arrangement allows getting a representative surface-to-volume ratio. A sump is located at the bottom of the vessel (as shown in Fig. 5). Evaporation rate was controlled through condensers temperature.

In order to avoid potential chemical interactions with the vessel walls, iodine was substituted for oxygen and acetaldehyde (C_2H_4O). Most of the tests were performed with oxygen. The gas was initially injected into the vessel atmosphere and its absorption in the sump was recorded along time throughout the experiments by measuring the aqueous concentration. Table 2 collects the major features of those experiments used for validation, all of them under evaporative conditions. Experiments with C_2H_4O were carried out but the associated uncertainties in the corresponding measurements made them unsuitable for validation purposes (Cantrel and March, 2006).

In addition to the aqueous concentration, other variables were monitored throughout the tests. The vessel thermal state was characterized by several thermocouples placed in the gas and liquid phases and at condenser surfaces, and by a pressure transducer. The oxygen partial pressure was also measured by three oxygen analyzers located at three different elevations (as shown in Fig. 5). The gas was permanently sampled and re-injected in the vessel via

Table 2
Conditions of the tests used for validation.

Test	V_ℓ (m^3)	A_{int} (m^2)	T_{gas} (°C)	T_ℓ (°C)	T_{cond} (°C)	$\dot{m}_{ev}$ (kg/s)
EV2	0.125	0.268	100.6	90.5	50.5	0.51×10^{-3}
EV3	0.125	0.268	108.0	118.5	96.0	1.07×10^{-3}
EV4	0.900	2.46	99.5	90.3	56.5	2.10×10^{-3}
EV5	0.720	2.46	98.3	89.8	55.7	2.00×10^{-3}

Table 3
Estimated mass transfer coefficients (in m/s) of SISYPHE experiments.

Test	k_ℓ	k_g
EV2	5.0×10^{-5}	4.2×10^{-3}
EV3	6.8×10^{-5}	2.3×10^{-3}
EV4	5.0×10^{-5}	4.4×10^{-3}
EV5	5.0×10^{-5}	4.5×10^{-3}

a heated loop. A rather detailed description of the facility and the test protocol may be found in (Cantrel, 2005a).

4.2. Simulation approach

The IODE module of ASTEC code (Cantrel, 2005b) includes a model for iodine mass transfer (Cantrel and March, 2006) which will be briefly described in Section 4.4. The ASTEC v1.2 code has been properly modified to get the new transfer model presented above (hereafter named CIEMAT model) implemented into the IODE module and to take into account those properties of oxygen that differ from iodine's ones. In particular, the oxygen partition coefficient at 90 and 120 °C has also been implemented (0.0216 and 0.0234, respectively) (Cantrel and March, 2006). As evaporation rate was experimentally recorded, it was used to estimate the value of the Sherwood number in Eq. (10) through the expression (Herranz et al., 2007):

$$Sh_{\mathrm{H2Ov}} = \frac{L}{A_{\mathrm{int}} D_{\mathrm{g,H2Ov}}} \frac{R T_{\mathrm{g}}}{P_{\mathrm{g}} M_{\mathrm{H2Ov}}} \ln\left(\frac{P_{\mathrm{nc}}^{\mathrm{bulk}}}{P_{\mathrm{nc}}^{\mathrm{int}}}\right) \dot{m}_{\mathrm{ev}} \tag{17}$$

The resulting mass transfer coefficients (Table 3) were given in the ASTEC-IODE input deck. It is worth noting that the experimental gas velocity was not measured. Nonetheless, as under thermal steady state condensation and evaporation rates matched each other during the tests (Cantrel, 2005a), if steam condensation is assumed to be the main driving force of gas motion, one obtains that gas velocity should have been encompassed within the 10^{-2} to 10^{-1} m/s range. Then, in order to estimate $k_{\ell,\mathrm{O2}}$, two different values of gas velocity, U, have been used: 10^{-2} and 5×10^{-2} m/s.

4.3. Comparison to data

The predictions of the CIEMAT model are presented in Fig. 6 along with data and ASTEC-IODE model estimates for the four tests considered (Cantrel, 2005a).

The oxygen evolution in the aqueous phase, both experimentally and theoretically, may be described by two stages: a first transient period in which concentration grows from a zero initial value, and then a slow-down of concentration rise until it eventually reaches a steady state. Generally speaking, both models follow the experimental trends.

Concerning the concentration growing period, it may be observed that CIEMAT model seems to accurately capture the transient behavior of the EV4 and EV5 tests when using the U upper value, whereas the best fitting to the EV3 results from the U lower value. This is consistent with the fact that in EV3 the pool surface was below the level of the hemispherical lower plenum of the vessel. Presumably, this would have partially hindered the gas–liquid tangential interaction with respect to the one in EV4 and EV5 (at which pool surface contacted the main body of the gas atmosphere). The EV2 also supports this explanation. Even though not so directly applicable because of deviations in the long-run, the EV2 transient behavior also indicates that gas velocity should have been less than 5×10^{-2} m/s during that experiment.

Therefore, the estimate of U range from steam condensation rate seems to be consistent (gas velocities being around 10^{-2} m/s) and, in addition, it should be expected that EV4 and EV5 gas velocities had been a bit higher than EV2 and EV3 ones. No specific value, however, can be attributed since the curve slope during the transient is also dependent on steady values of concentration.

Table 4
Steady state values of oxygen aqueous concentration (in 10^{-3} kg/m^3).

Test	Data	ASTEC		CIEMAT	
	C_ℓ	C_ℓ	Error (%)	C_ℓ	Error (%)
EV2	2.46	2.75	11.9	2.24	9.1
EV3	2.31	2.39	3.5	2.21	4.3
EV4	4.66	4.47	4.1	3.84	17.6
EV5	4.79	4.19	12.5	3.63	24.2

Fig. 6 shows that CIEMAT model always underestimates the concentration asymptotic value measured (experimental error being around 10%). A quantitative analysis of those deviations (Table 4) indicates that they range from around 5 to 25%. These errors are considered more than acceptable for the mechanistic approach proposed, since it relies on assumptions such as the heat-mass transfer analogy which accuracy is roughly characterized by that same interval (Herranz and Campo, 2002).

Therefore, the CIEMAT model performance can be considered highly satisfactory. On one side, it reaches the highest feasible accuracy given its grounds and hypotheses. On the other, the model uncertainty is negligible when compared to the overall uncertainty affecting in-containment gaseous iodine inventory during postulated severe accidents—some of the most contributing processes being organic iodine chemistry or iodine interactions with surfaces (Clément et al., 2007).

4.4. Comparison to the ASTEC model

The ASTEC model assumes that evaporation affects iodine flow rate both at the gas and at the aqueous phase. So, the base equations are (Cantrel and March, 2006):

$$\varphi_{\mathrm{g}} = A_{\mathrm{int}} k_{\mathrm{g}} (C_{\mathrm{g}} - C_{\mathrm{g}}^{\mathrm{int}}) + \alpha \frac{\dot{m}_{\mathrm{ev}}}{\rho_{\mathrm{sat}}(P_{\mathrm{g}})} C_{\mathrm{g}}^{\mathrm{int}} \tag{18}$$

$$\varphi_\ell = A_{\mathrm{int}} k_\ell (C_\ell^{\mathrm{int}} - C_\ell) + \beta \frac{\dot{m}_{\mathrm{ev}}}{\rho_\ell} C_\ell^{\mathrm{int}} \tag{19}$$

where α and β are parameters estimated by fitting the SISYPHE experimental data (0.19 and 6.6, respectively). This different basis yields a final flow rate expression well other than Eq. (6):

$$\varphi = A_{\mathrm{int}} \left(\frac{k_{\mathrm{g}} k_\ell}{k_{\mathrm{g}} + H k_\ell + \alpha(\dot{m}_{\mathrm{ev}}/(A_{\mathrm{int}} \rho_{\mathrm{sat}}(P_{\mathrm{g}}))) - \beta(\dot{m}_{\mathrm{ev}}/(A_{\mathrm{int}} \rho_\ell)) H} \right) \times \left[\left(1 - \beta \frac{\dot{m}_{\mathrm{ev}}}{A_{\mathrm{int}} \rho_\ell k_\ell}\right) H C_{\mathrm{g}} - \left(1 + \alpha \frac{\dot{m}_{\mathrm{ev}}}{A_{\mathrm{int}} \rho_{\mathrm{sat}}(P_{\mathrm{g}}) k_{\mathrm{g}}}\right) C_\ell \right] \tag{20}$$

And at equilibrium ($\varphi = 0$), the concentration ratio is also different from Eq. (7):

$$\frac{C_\ell}{C_{\mathrm{g}}} = H \left(\frac{1 - \beta(\dot{m}_{\mathrm{ev}}/(A_{\mathrm{int}} \rho_\ell k_\ell))}{1 + \alpha(\dot{m}_{\mathrm{ev}}/(A_{\mathrm{int}} \rho_{\mathrm{sat}}(P_{\mathrm{g}}) k_{\mathrm{g}}))} \right) \tag{21}$$

Likewise, mass transfer coefficients are estimated through other equations than those proposed in the CIEMAT model: k_{g} uses a mass transfer correlation obtained for vertical plates with very low solute concentration and low transfer velocity for turbulent flow; and k_ℓ is based on the surface renewal theory but introducing an enhancement factor accounting for evaporative conditions.

As observed in Fig. 6 and Table 3, the CIEMAT model behaves rather similarly to the ASTEC one, slightly worse though. As both models are based on the two-film diffusion model, their consistency with experimental trends underlines suitability of this approach.

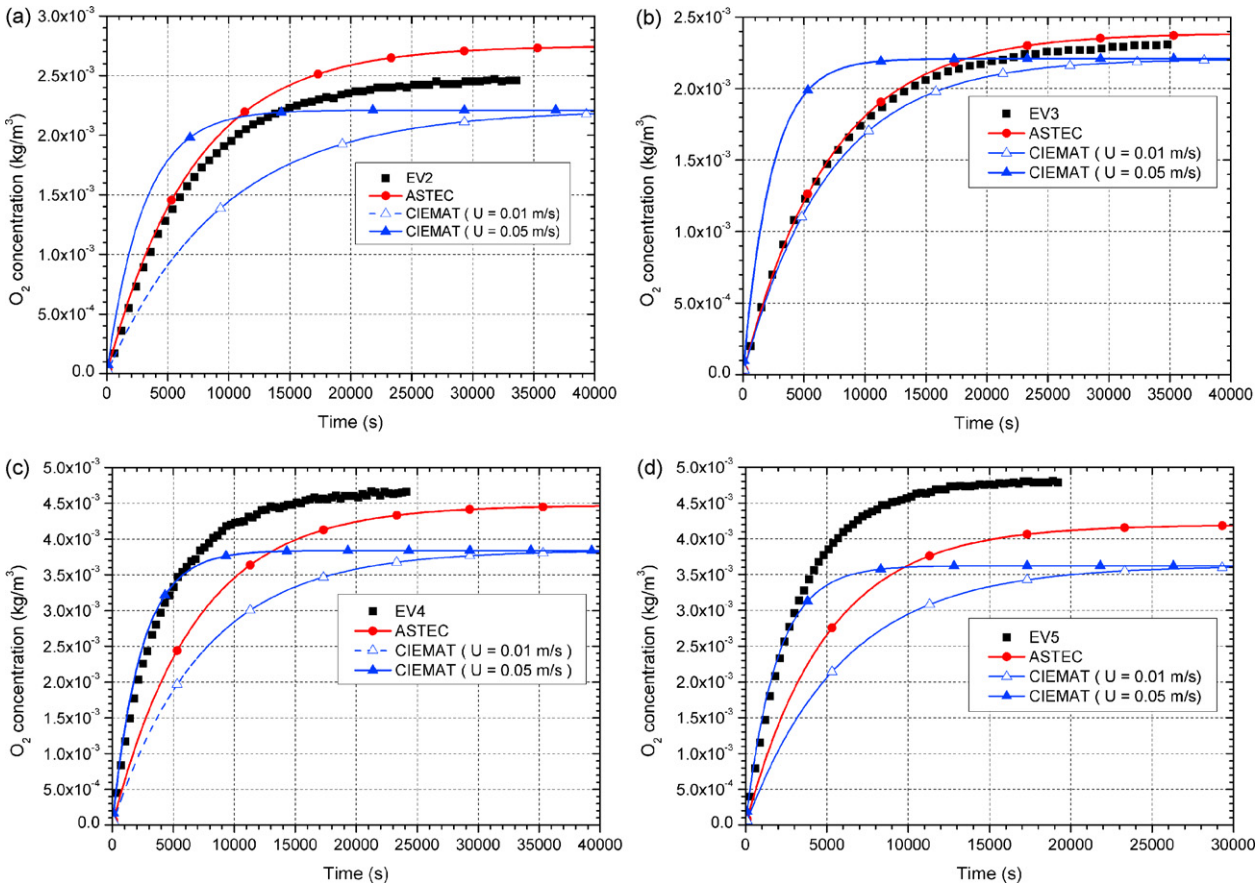

Fig. 6. Aqueous oxygen concentration in the SISYPHE experiments.

The better performance of the IRSN model stems from its semi-empirical nature. The model includes two parameters (α and β) resulting from fitting predictions to the SISYPHE data (Cantrel, 2005a). They modulate the effect of evaporation on the gaseous mass flow rate ($\alpha = 0.19$) and on the liquid mass flow rate ($\beta = 6.6$). In addition, its predictions, although generally more accurate than the CIEMAT ones, are not always conservative and stand over data in some occasions (i.e., EV2 and EV3).

5. Conclusions and further work

Once the potential impact of evaporative conditions on gaseous iodine inventory has been illustrated, the major features of an iodine mass transfer model from aqueous-to-gaseous phases have been presented. Even though hypotheses and assumptions are needed, the model fundamentals are based on well-credited theoretical developments: the two-film model to estimate iodine diffusion, the heat-mass transfer analogy to derive gas mass transfer coefficients and the surface renewal theory to approximate liquid mass transfer coefficients.

The model has been compared to a set of data from the SISYPHE program in which boundary conditions were representative of post-accident conditions in containment. The model behaved rather accurately yielding errors between 5 and 25% in the long-term aqueous concentration of oxygen (iodine substitute) and slopes with a noticeable qualitative consistency with data. Such accuracy is considered very satisfactory for a model which does not rely on any empirical parameter. As compared to the model used in the ASTEC code at present, the so called CIEMAT model presents three major advantages: it is not fitted to any specific data set; although precise, estimates are always conservative; and, no less important, its bases, as well as hypotheses, are thoroughly documented.

The model bases seem suitable for application to more complex system modeling for real iodine behavior (i.e., wall effects, organic compounds, gas-phase reaction, etc.). Nonetheless, the model is far from having been submitted to an extensive validation. Available data are scarce, but as soon as further representative data become available model validation should be continued, preferably against data from large scale experiments involving iodine.

Acknowledgments

The authors appreciate the SARNET framework through which the experimental information used in this paper was available and acknowledge P. March (IRSN) for the fruitful discussions concerning experimental aspects.

References

Cantrel, L., 2005. Interpretation of SISYPHE experiments—mass transfer modelling with and without evaporation in IODE module of ASTEC. SARNET report SARNET-ST-P14. IRSN Technical Note: IRSN/DPAM/SEMIC/2004-01.
Cantrel, L., June 2005. ASTEC v1.2—IODE module: iodine behaviour in containment. Technical Note SEMIC-2005-0167.
Cantrel, L., March, P., 2006. Mass transfer modeling with and without evaporation for iodine chemistry in the case of a severe accident. Nucl. Technol. 154, 170–185.
Clément, B., Cantrel, L., Ducros, G., Funke, F., Herranz, L.E. Rydl, A., Weber, G., Wren, C., 2007. State of the art report on iodine chemistry. NEA/CSNI/R(2007)1.
Cohen, Y., 1983. Mass transfer across a sheared, wavy air–water interface. Int. J. Heat Mass Transf. 26 (9), 1289–1297.
Cohen, Y., Cocchio, W., Mackay, D., 1978. Laboratory study of liquid-phase controlled volatilization rates in presence of wind waves. Am. Chem. Soc. 12 (5), 553–558.
de la Rosa, J.C., Escrivá, A., Herranz, L.E., Cicero, T., Muñoz-Cobo, J.L., 2009. Review on condensation on containment structures. Prog. Nucl. Energy 51 (1), 32–66.

Emerson, S., 1975. Gas exchange in small canadian shield lakes. Limnol. Oceanogr. 20 (5), 745–761.
Green, J., Almenas, K., 1996. An overview of the primary parameters and methods for determining condensation heat transfer to containment structures. Nucl. Saf. 37, 26–47.
Haste, T., Giordano, P., Herranz, L.E., Micaelli, J.-C., 2006. SARNET: integrated severe accident research in Europe—safety issues in the source term area. In: Proceedings of the International Congress on Advances in Nuclear Power Plants, ICAPP '06, Reno, USA, June 4–8.
Herranz, L.E., Campo, A., 2002. Adequacy of heat-mass transfer analogy to simulate containment atmospheric cooling in the new generation of advanced nuclear reactors: experimental confirmation. Nucl. Technol. 139, 221–232.
Herranz, L.E., Vela-García, M., Fontanet, J., López del Prá, C., 2007. Experimental interpretation and code validation based on the PHEBUS-FP programme: lessons learnt from the analysis of the containment scenario of FPT1 and FPT2 tests. Nucl. Eng. Des. 237, 2210–2218.
Incropera, F.P., Dewitt, D.P., 2002. Fundamentals of Heat and Mass Transfer, 5th ed. John Wiley & Sons (Chapter 9).
IRSN, CEA, EDF, 2004. Proposal for a Cooperative Research Programme on Severe Accidents: Source Term Separate Effect Tests Programme.
Kanwisher, J., 1963. On the exchange of gases between the atmosphere and the sea. Deep-Sea Res. 10, 195–207.
Perry, R.H., Green, D.W., 1997. Perry's Chemical Engineers' Handbook, 7th ed. McGraw-Hill.
Reid, R.C., Prausnitz, J.M., Poling, B.E., 1988. The Properties of Gases & Liquids, 4th ed. McGraw-Hill.
Schwarz, M., Zeyen, R., 2003. Status of the PHEBUS-FP program. In: Proceedings of the 5th Technical Seminar on the PHEBUS-FP Programme, Aix-en-Provence, June 24–26.
Shepherd, I., Jones, A.V., Gaillot, S., Herranz, L.E., Akagane, K., 1995. Thermal-hydarulics testing of the PHEBUS-FP containment. In: Proceedings of the International Symposium on Heat and Mass Transfer on Severe Nuclear Reactor Accidents, Kusadasi, Turkey, May 22–26.
Van Dorsseleare, J.P., Schwinges, B., June 2005. Overview of the integral code ASTEC V1.2. IRSN Technical Note DPAM/ASTEC-2005-182, GRS Technical Note GRS ASTEC 05/04.
Verloo, E., Jacquemain, D., Spitz, P., 1998. SISPYPHE: description of the facility and presentation of the thermal hydraulic and mass transfer programme. Technical Note IPSN/DRS/SESHP No. 98-883.
Wu, J., 1980. Wind-stress coefficients over sea-surface near neutral conditions—a revisit. J. Phys. Oceanogr. 10, 727–740.